Available online at www.sciencedirect.com
ScienceDirect
Polymer 49 (2008) 952–956
polymer
www.elsevier.com/locate/polymer

# Flow analysis of aqueous solution of silk fibroin in the spinneret of *Bombyx mori* silkworm by combination of viscosity measurement and finite element method calculation

Motoaki Moriya [a], Kosuke Ohgo [b], Yuichi Masubuchi [c], Tetsuo Asakura [b,*]

[a] *Department of Applied Chemistry, Tokyo University of Agriculture and Technology, Koganei, Tokyo 184-8588, Japan*
[b] *Department of Biotechnology, Tokyo University of Agriculture and Technology, Koganei, Tokyo 184-8588, Japan*
[c] *Institute for Chemical Research, Kyoto University, Uji, Kyoto 611-0011, Japan*

Received 26 September 2007; received in revised form 20 December 2007; accepted 21 December 2007
Available online 3 January 2008

**Abstract**

*Bombyx mori* silk fibers possess outstanding mechanical properties in spite of being spun at room temperature and from the aqueous solution. Therefore, the mechanism of the structural transition has been studied with great attention, but still not be well understood. In this study the flow simulation of the silk fibroin aqueous solution using finite element method was performed on the basis of both the relationship between the viscosity and shear rate of the silk fibroin solution prepared from the silk gland, and the detailed structure of the spinneret including silk press part of the silkworm obtained from the optical micrographs. The viscosity of the silk fibroin solution decreased with power-law till the shear rate, about 1.5 $s^{-1}$ with increasing shear rate. Then the viscosity increased reversely which is speculated due to the fiber formation as a result of aggregation of the molecules. In the flow simulation analysis, the initiation site of the fiber formation was calculated by regulating the extrusion pressure. The fiber formation occurs in 550 μm from the spigot at 1 MPa and in 600 μm from the spigot at 50 MPa. The extrusion pressure in the range from 1 MPa to 50 MPa induces the fiber formation in the stiff plates (550–600 μm from the spigot), that is, the silk press part in the spinneret.


*Keywords:* Fiber formation of *Bombyx mori* silk fibroin; Structure of the spinneret of silkworm; Flow analysis with finite element method

## 1. Introduction

It is well known that silk fibroin fibers from *Bombyx mori* exhibit exceptional strength, toughness, and resistance to mechanical compression although the silkworm produces the fibers at room temperature and from an aqueous solution [1,2]. The mechanism of the structural transition has been studied with great attention, but still not been well understood. It has been reported that the silk fibroin protein exhibits structural change [3] from Silk I [4] to Silk II [5] during the spinning process in the spinneret and the structural change has been investigated by birefringence [6], for example. Also rheological properties of the aqueous solution of the silk fibroin have been studied for understanding the fiber formation mechanism. Kataoka and Uematsu [7] reported flow behavior of the aqueous solution of the silk fibroin by assuming that it is a Newtonian fluid. Holland et al. [8,9] and Terry et al. [10] reported that the silk fibroin solution shows shear thinning behavior found in polymer solutions. Ochi et al. [11,12] reported dynamic viscoelasticity of silk fibroin solution prepared from the silk glands.

The conventional studies on the fiber formation process are, however, not enough to reveal the spinning process since the fiber formation essentially occurs in the spinneret of silkworm *in vivo*. An approach on the basis of the structure of the spinneret including silk press part where the silk fibroin molecules are filled and flow is required.

The present study aims to perform flow simulation analysis using finite element method (FEM) to clarify the fiber formation

* Corresponding author. Tel./fax: +81 42 383 7733.
*E-mail address:* asakura@cc.tuat.ac.jp (T. Asakura).

0032-3861/$ - see front matter © 2007 Elsevier Ltd. All rights reserved.
doi:10.1016/j.polymer.2007.12.032

mechanism in the spinneret. The detailed structure of *B. mori* spinneret was reconstructed from the optical micrographs obtained in our previous study [13]. FEM calculation has been frequently used for flow analyses in the biological/medical fields such as aneurysm [14] because the calculation possesses the benefit that can reflect the intricacy of the model. For the simulation, the viscosity of the aqueous solution of silk fibroin prepared from the middle silk glands was measured as a function of the shear rate. Through the simulation results, the fiber formation of silk fibroin shall be discussed on the initiation site of the fiber formation, the extruded pressure, the flow velocity and so on.

## 2. Experimental

### 2.1. Sample preparation and viscosity measurement

The aqueous solution of silk fibroin was obtained from the middle silk glands of the fifth instar larval stage of *B. mori* as follows. The middle silk gland division was cut out from other divisions by a pair of scissors and then immersed in the distilled water. The thin epithelial surface as well as hydrophilic sericin layer was removed carefully by a pair of forceps [11,12]. The concentration of the obtained fibroin aqueous solution is around 25 wt%. Viscosity of the solution at 25 °C was measured with a rotational stress controlled rheometer, Physica MCR-301 purchased from AntonPaar Co. Inc. equipped with a disposable parallel plate type jig with diameter of 25 mm and gap of 0.3 mm to eliminate possible contaminations. The steady shear viscosity was measured in the shear rate range of 0.1–100 $s^{-1}$. All measurements were repeated three times and the average of these data was employed for the FEM calculations. We interchanged the sample with respect to each measurement.

### 2.2. Model construction for the calculation

The 3D structural model of the channel in the spinneret for the FEM calculation was constructed from the sliced optical micrographs obtained previously [13]. Structure of the canal wall of the spinneret was extracted from the 83 micrographs at interval of 10 μm by a computer code called TRI/3D-SRFII (RATOC System Engineering Co. Inc., Japan) and converted into triangular lattice surface elements. The duct model in the spinneret was then filled with 180,000 tetrahedron lattice elements by another computer code called FEPartner (PLAMEDIA Co. Inc., Japan).

### 2.3. Flow simulations

Flow profile in the spinneret in steady state under given pressure difference between inlet and outlet was calculated by solving incompressible Navier–Stokes equation with assumptions where (i) the temperature is homogeneous and set to be constant at 25 °C, (ii) the fluid is purely viscous with non-Newtonian shear viscosity, (iii) solidification (or fiber formation) is not considered in the calculation, (iv) the fluid and the wall are in non-slip contact and (v) the contraction motion of the spinneret during spinning is neglected. The viscosity was obtained by the measurement described above. The density of the fluid was fixed at $\rho = 1.36$ g/cm$^3$ [15]. The examined pressure difference was ranged from 0.0170 MPa to 200 MPa. The calculation was performed by a computer code called SUNDY TETRA (PLAMEDIA Co. Inc., Japan).

## 3. Results and discussion

### 3.1. Flow curve

Fig. 1 shows a flow curve of the fibroin solution. The corresponding data reported by other researchers are also shown [8–10]. The decrease in viscosity with increasing the shear rate in the range of 0.1–1.5 $s^{-1}$ is characterized as shear thinning behavior and is similar to the phenomena observed in polymer solutions [16]. Concerning the shear thinning behavior it is also noted that silk fibroin solution from the mature silkworm possesses a character of liquid–crystal sol [17,18] which indicates similar behavior [19,20].

After indicating a bottom at a certain critical shear rate around 1.5 $s^{-1}$, the viscosity increased abruptly because of the agglutinate of silk fibroin. The measurement was interrupted before reaching to 100 $s^{-1}$ because the agglutinate of silk fibroin induced by shear stress disturbed the rotation of the jig.

It is noted that the increase of the viscosity was not observed in the study by Holland et al. [8]. It was reported that in their measurement the shear rate higher than 2–5 $s^{-1}$ led to instability of dope, which first turned into an opaque, white solid and was then ejected from the measuring geometry [8]. In our measurement the ejection of the sample was not observed. We speculate that the ejection induced the difference in the viscosity but detail mechanism is unknown. It is also noted that the critical shear rate measured in our study is consistent with the calculated critical shear rate (1.2 $s^{-1}$) by Kataoka and Uematsu [6] and is also similar to the shear rate where the white solid appeared in the measurement by Holland et al. [8]. On comparison of the data it is noted that the employed geometry in our experiments was the parallel plate while in the experiments by Holland

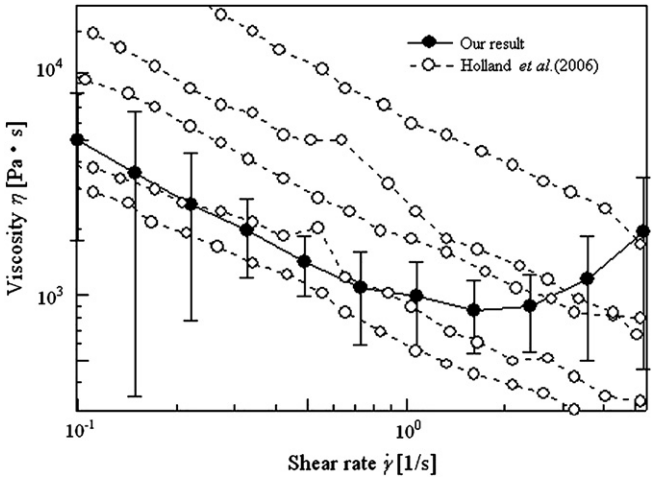


Fig. 1. Flow curve of raw silk fibroin solution. The results by Holland et al. [8] are also shown for comparison. Values are average ± standard deviation of three measurements.

et al. [8], for example, the cone plate geometry was used. Due to the non-Newtonian nature of the material the artifacts caused by the geometry may affect the results though the results in Fig. 1 shows reasonable consistency among the data.

For the flow simulation a mathematical description of the measured flow curve was constructed. It is apparent that the shear thinning behavior before the critical shear rate follows a power-law trend expressed by $\eta = a\dot{\gamma}^n$, where $\eta$ is viscosity and $\dot{\gamma}$ is shear rate. $a$ and $n$ are fitting constants and the best fit gives $a = 1.0 \times 10^3$ and $n = -0.65$. After the critical shear rate the increasing behavior of the viscosity can be described by $\eta = b\dot{\gamma}^m + c$ where $b$, $c$ and $m$ are fitting constants. From the best fit of the data we obtain $b = 9.0$, $m = 2.9$ and $c = 7.5 \times 10^2$. To escape from numerical difficulty the viscosity was assumed being constant below 0.1 $s^{-1}$ and above 10 $s^{-1}$.

### 3.2. The structure of the duct in the spinneret and stiff plates

The 3D structure of the spinneret is shown in Fig. 2 with several cross-sectional micrographs used to reconstruct the 3D model. From the 3D model, it is possible to describe the feature of the spinneret anatomically. The spinneret of *B. mori* silkworm has the complicated duct. Briefly the duct of the spinneret is not flat and the diameter of the duct changes, depending on the distance from the spigot. Additionally, the stiff plates which are made up of chitin exist with pinching the duct of the spinneret as indicated in Fig. 3. The stiff plates in upper and lower lip sides are located in 380–600 μm and 550–600 μm from the spigot, respectively.

In order to know the change in the diameter of the duct against the location of stiff plates, the cross-sectional area was calculated as a function of the distance from the spigot (Fig. 3). The value of the cross-sectional area drastically decreases around 600 μm. This site coincides with the location

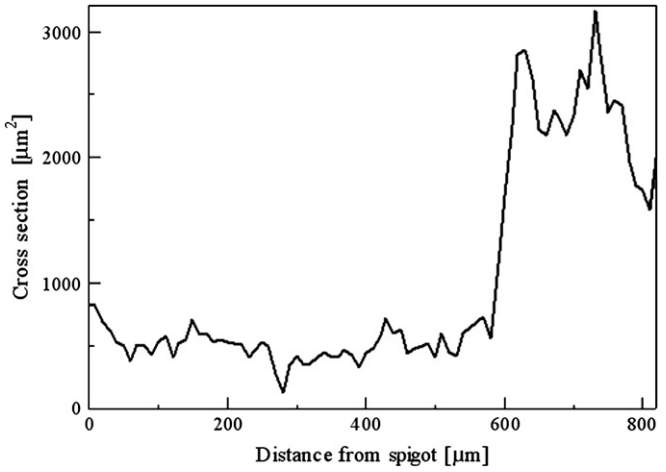


Fig. 3. Changes in the cross-sectional area (μm²) of the duct in the spinneret as a function of the distance from the spigot.

where the stiff plates begin to appear. The location of the stiff plates indicates that the stiff plates squeeze the duct and besides silk fibroin may undergo large external force in this area.

It is suggested that features of raw silk fibroin appear depending on the location of the stiff plates. One of the examples is change in the birefringence corresponding to the change of molecular configuration. It abruptly increases near a boundary between silk press part and common tube in the spinneret [6]. Furthermore this site accords with the initiation site where stiff plates appear in our model namely at 600 μm.

### 3.3. Flow analysis

As described above, it is meaningful to focus attention on the change in the shear rate at the location of the stiff plates on the simulation. The spinning processes of silkworms rely on the complicated duct and the extrusion process [8]. Thus

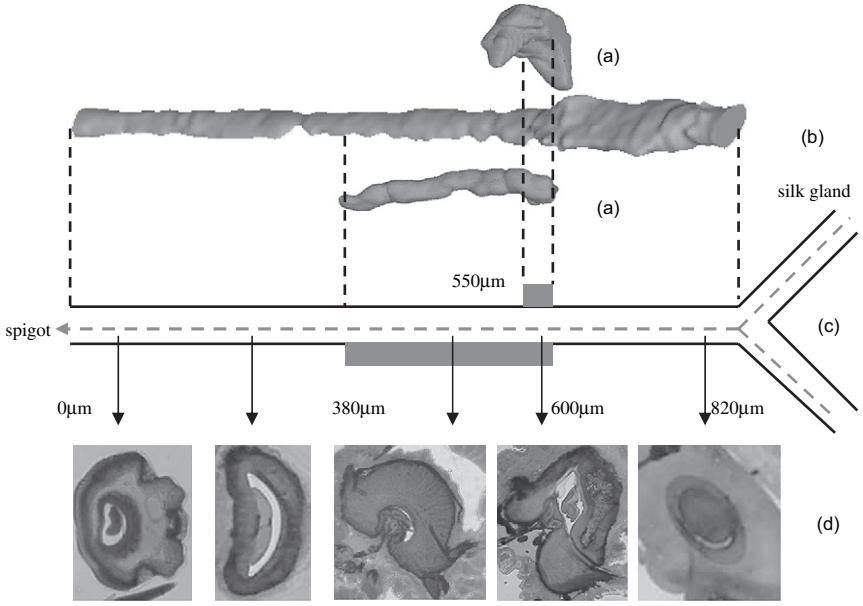


Fig. 2. The structure of the flow channel in the spinneret. (a) The mature silkworms possess the stiff plates in the spinneret. (b) The duct of spinneret exhibits taper. (c) Simplified pictures of the flow path in the spinneret. (d) Optical micrographs of the spinneret corresponding with each section of the flow path.

it is important to evaluate several parameters such as shear rate profile and extrusion pressure in order to develop a better understanding of the spinning of the silkworms. As an example of the simulations, Fig. 4 shows the profile of shear rate at 5 MPa. Other profiles under different pressures have similar trend except for different absolute values. The fiber formation was judged by the critical shear rate of 1.5 $s^{-1}$. The initiation site of the fiber formation was defined as a circle (580 μm) as shown in Fig. 4. In Table 1, the results of simulation at each regulated pressure are summarized.

It is known that silk fibroin has large shear stress at the stiff plates. The value of shear rate in the spinneret changes depending on the extrusion pressure. The extrusion pressure for the fiber formation in the location of stiff plates was researched. The fiber formation of silk fibroin arises at 550–600 μm (namely the site of the stiff plates) in the pressure range of 1–50 MPa. Briefly the result indicates that the structure of silk fibroin undergoes change from Silk I to Silk II at the site in this pressure range.

The flow volume had been calculated from the spinning rate of silkworms by Tsubouchi [21] as $1.66 \times 10^{-3}$ $mm^3/s$. We regulated the extrusion pressure corresponding to the valuated flow volume and performed the flow simulation. The extrusion pressures which reaches the valuated flow volume was 200 MPa as listed in Table 1. However, the fiber formation occurs at once in this condition namely the shear rate is over 1.5 $s^{-1}$ at the beginning of the flow because the extrusion pressure was regulated as unusually large. This result indicated that these pressures and flow volumes do not conform to those of silkworms.

Additionally we examined simulation at both blood pressure (0.0170 MPa) as an *in vivo* pressure and atmospheric pressure (0.100 MPa). In these cases, the fiber formation is not able to arise because of their lower extrusion pressure.

Table 1
The information for the fiber formation at each extrusion pressure

| Pressure difference, $\Delta P$ [MPa] | Flow volume, $Q$ [$mm^3/s$] | Initiation site of fiber formation on the central flow, $f_{\Delta P}$ [μm] | Maximum velocity, $V_{max}$ [μm/s] | Average velocity, $V_{ave}$ [μm/s] |
|---|---|---|---|---|
| 0.0170[a] | $1.8 \times 10^{-7}$ | –[c] | $1.9 \times 10^{-1}$ | $5.8 \times 10^{-2}$ |
| 0.100[b] | $1.5 \times 10^{-6}$ | –[c] | 1.7 | $5.1 \times 10^{-1}$ |
| 1.00 | $1.6 \times 10^{-5}$ | 550 | $1.8 \times 10$ | 5.3 |
| 3.00 | $4.5 \times 10^{-5}$ | 560 | $4.9 \times 10$ | $1.5 \times 10$ |
| 5.00 | $6.6 \times 10^{-5}$ | 580 | $7.1 \times 10$ | $2.2 \times 10$ |
| 15.0 | $1.2 \times 10^{-4}$ | 580 | $1.3 \times 10^{2}$ | $4.1 \times 10$ |
| 30.0 | $2.0 \times 10^{-4}$ | 590 | $2.1 \times 10^{2}$ | $6.3 \times 10$ |
| 50.0 | $2.8 \times 10^{-4}$ | 600 | $3.2 \times 10^{2}$ | $9.9 \times 10$ |
| 200 | $1.2 \times 10^{-3}$ | –[d] | $1.3 \times 10^{3}$ | $3.8 \times 10^{2}$ |

[a] Corresponds to a blood pressure of 130 mmHg.
[b] Corresponds to atmospheric pressure of 1 hPa.
[c] The shear rate is under 1.5 $s^{-1}$ through the spinneret.
[d] The shear rate is over 1.5 $s^{-1}$ at the beginning of the flow.

In these simulations, it is indicated that silk fibroin is not able to flow on *in vivo* or atmospheric pressures.

The present study elucidates the range of the extrusion pressure which induces the fiber formation at stiff plates. This range disaccord with *in vivo* pressure and it is an issue in the future.

## 4. Conclusion

The 3D model of the spinneret showed that the stiff plates existed in the range of 550–600 μm from the spigot. The flow curve of silk fibroin showed that silk dope underwent the shear thinning in the range of 0.1–1.5 $s^{-1}$ and the shear thickening over 1.5 $s^{-1}$ in contrast. The flow simulations clarified the range of extrusion pressure of 1–50 MPa for the fiber

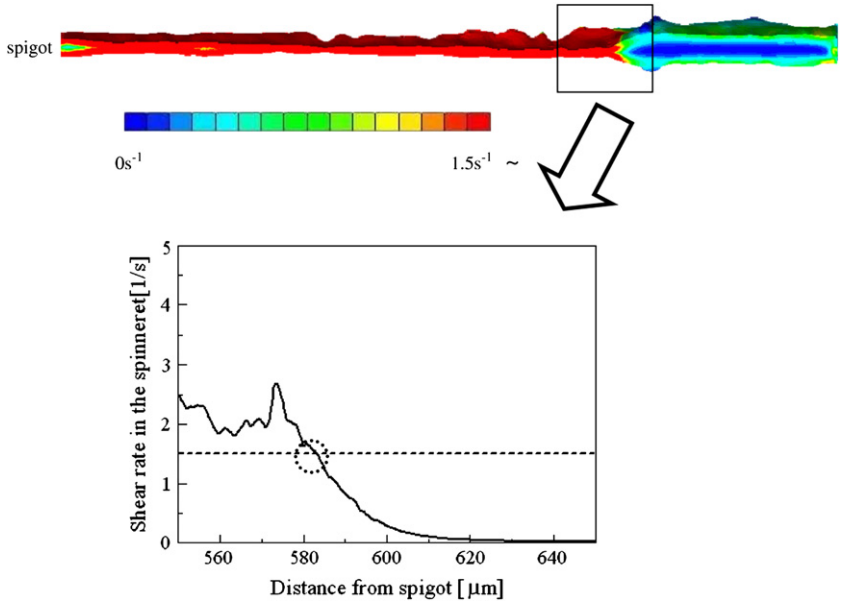


Fig. 4. Shear rate profile in the spinneret at 5 MPa. The shear rate along the central line is plotted against the distance from the spigot and shown below. Dotted line and circle show a critical shear rate (1.5 $s^{-1}$) and the initiation site of the fiber formation.

formation of silk fibroin at the location of the stiff plates. This extruder pressure might approach *in vivo* pressure by considering the effects of metal ion, pH [22,23], and sericin [24]. It is noted that in the flow simulations we did not take into account the effect of elasticity of the fluid as well as deformation of the spinneret because of computational limitations as mentioned in Section 2.3. Since these assumptions may have some effects on the results, supplemental studies have been performed and the results will be published elsewhere. Additionally the results of our simulation might contribute to make functional biomimetic extruder.

## Acknowledgments

T.A. acknowledges support from Grants-in-Aid for Scientific Research (S) (No. 18105007), Japan. We would like to acknowledge Mr. Y. Nakahara at PLAMEDIA Co. Inc. for FEM calculation and Mr. S. Nango at RATOC System Engineering Co. Inc. for manufacture of model.

## References

[1] Asakura T, Kaplan DL. In: Arutzen CJ, editor. Encyclopedia of agricultural science, vol. 4. New York: Academic Press; 1994. p. 1–11.
[2] Shao ZZ, Vollrath F. Nature 2002;418(6899):741.
[3] Yamane T, Umemura K, Nakazawa Y, Asakura T. Macromolecules 2003; 36(18):6766–72.
[4] Asakura T, Ashida J, Yamane T, Kameda T, Nakazawa Y, Ohgo K, et al. J Mol Biol 2001;306(2):291–305.
[5] Asakura T, Yao JM, Yamane T, Umemura K, Ultrich AS. J Am Chem Soc 2002;124(30):8794–5.
[6] Kataoka K, Uematsu I. Kobunshi Ronbunshu 1977;34:457–64.
[7] Kataoka K, Uematsu I. Kobunshi Ronbunshu 1977;34:7–13.
[8] Holland C, Terry AE, Porter D, Vollrath F. Nat Mater 2006;5(11):870–4.
[9] Holland C, Terry AE, Porter D, Vollrath F. Polymer 2007;48(12):3388.
[10] Terry AE, Knight DP, Porter D, Vollrath F. Biomacromolecules 2004; 5(3):768–72.
[11] Ochi A, Nemoto N, Magoshi J, Ohyama E, Hossain KS. J Soc Rheol Jpn 2002;30(5):289–94.
[12] Ochi A, Hossain KS, Magoshi J, Nemoto N. Biomacromolecules 2002; 3(6):1187–96.
[13] Asakura T, Umemura K, Nakazawa Y, Hirose H, Higham J, Knight D. Biomacromolecules 2007;8(1):175–81.
[14] Yamamoto S, Maruyama S, Nakahara Y, Yoneyama S, Tanifugi S, Wada S, et al. Jpn J Radiol Tech 2006;62:115–21.
[15] Kataoka K, Uematsu I. Kobunshi Ronbunshu 1977;34:37–41.
[16] Ferry JD. Viscoelastic properties of polymers. 3rd ed. New York: Wiley and Sons; 1980.
[17] Magoshi J, Magoshi Y, Nakamura S. Polym Commun 1985;26(2):60–1.
[18] Guangxian L, Tongyin Y. Macromol Rapid Commun 1989;10(8):387–9.
[19] Atul Mehta II A. Polym Eng Sci 1991;31(13):971–80.
[20] Burghardt WR, Fuller GG. Macromolecules 1991;24(9):2546–55.
[21] Tsubouchi K. Bull Sericul Exp Sta 1986;30:375–95.
[22] Foo CWP, Bini E, Hensman J, Knight DP, Lewis RV, Kaplan DL. Appl Phys A Mater Sci Process 2006;82(2):223–33.
[23] Chen X, Knight DP, Vollrath F. Biomacromolecules 2002;3(4):644–8.
[24] Magoshi J, Magoshi Y, Nakamura S. Sen'i Gakkaishi 1997;53(3): P87–97.